

Ultrahigh Energy Cosmic Rays from Topological Defects — Cosmic Strings, Monopoles, Necklaces, and All That¹

Pijushpani Bhattacharjee²

*Laboratory for High Energy Astrophysics,
NASA/Goddard Space Flight Center, Code 661,
Greenbelt, MD 20771. USA.*

and

*Indian Institute of Astrophysics
Koramangala, Bangalore 560 034, INDIA*

Abstract

The topological defect scenario of origin of the observed highest energy cosmic rays is reviewed. Under a variety of circumstances, topological defects formed in the early Universe can be sources of very massive particles in the Universe today. The decay products of these massive particles may be responsible for the observed highest energy cosmic ray particles above 10^{20} eV. Some massive particle production processes involving cosmic strings and magnetic monopoles are discussed. We also discuss the implications of results of certain recent numerical simulations of evolution of cosmic strings. These results (which remain to be confirmed by independent simulations) seem to show that massive particle production may be a generic feature of cosmic strings, which would make cosmic strings an inevitable source of extremely high energy cosmic rays with potentially detectable flux. At the same time, cosmic strings are severely constrained by the observed cosmic ray flux above 10^{20} eV, if massive particle radiation is the dominant energy loss mechanism for cosmic strings.

Introduction

Cosmic Topological Defects (TDs)[1, 2] such as magnetic monopoles, cosmic strings, domain walls, and various hybrid TD systems consisting of these basic kinds of TDs, are predicted to form in the early Universe as a result of symmetry-breaking phase transitions envisaged in unified theories of elementary particle interactions. Under a variety of circumstances these TDs can be sources of extremely massive unstable particles in the universe today[3, 4, 5, 6, 7, 8, 9, 10, 11]. The masses m_X of these so-called “X” particles (the quanta of

¹Invited talk given at the Workshop on “Observing the Highest Energy Particles ($> 10^{20}$ eV) from Space”, College Park, Maryland, USA, November 13 – 15, 1997, to be published in the Proceedings (AIP).

²NAS/NRC Resident Senior Research Associate at NASA/GSFC on sabbatical leave from Indian Institute of Astrophysics, Bangalore-560 034. India.

the massive gauge- and higgs fields of the underlying spontaneously broken gauge theory) would typically be of order the symmetry-breaking energy scale at which the relevant TDs were formed, which, in Grand Unified Theories (GUTs), can be as large as $\sim 10^{16}$ GeV. The decay of these X particles can give rise to extremely energetic photons, neutrinos and nucleons with energy up to $\sim m_X$. If the X particle production rate from TDs is large enough, these extremely energetic particles may be detectable by ground-based as well as space-based large-area detectors being planned for detecting ultrahigh energy (UHE) (i.e., energy $\gtrsim 10^9$ GeV) cosmic rays. These cosmic ray detectors may thus provide us with a tool for studying the signature of TDs and thus of GUT scale physics.

There is currently much interest in the possibility that the Extremely High Energy (EHE) Cosmic Ray (EHECR) events — those with energies above 10^{11} GeV reported recently[12] — may be due to decays of massive X particles originating from TDs[13, 10, 14, 15, 16, 17, 11]. This possibility is of interest in view of the fact that the energies associated with the EHECR events are hard to obtain[18, 13, 19] within the standard diffusive shock acceleration mechanism[20] that involves first-order Fermi acceleration of charged particles at relativistic shocks associated with known powerful astrophysical objects; see, however, Ref. [21]. In addition, there is the problem of absence of any obviously identifiable sources for these EHECR events[22, 13]. These problems are avoided in the TD scenario in a natural way. Firstly, no acceleration mechanism is needed: The decay products of the X particles have energies up to $\sim m_X$ which can be as large as, say, 10^{16} GeV. Secondly, the absence of obviously identifiable sources is not a problem because TDs need not necessarily be associated with any visible or otherwise active astrophysical objects such as AGNs or radio galaxies.

The basic ideas of the TD scenario of origin of EHECR have been reviewed in a number of discussions in the past; see, e.g., Refs. [7, 23, 24, 25]. Detailed calculations of the predicted spectra of nucleons, photons, and neutrinos in the TD scenario have been done in the past several years[3, 26, 10, 15, 14, 17, 16, 27]. Constraints on the TD scenario imposed by experimental data on EHECR and diffuse gamma ray background have also been discussed[28, 15, 17, 16].

In what follows, I first discuss briefly some of the basic aspects of topological defects and their formation in the early Universe. The basic steps in the calculation of the ‘observable’ particle spectra resulting from the decay of the X particles is discussed. A simple benchmark calculation of the X particle production rate required to explain the observed EHECR particle flux is performed. I then discuss three specific X particle production mechanisms involving (1) “ordinary” cosmic strings, (2) monopoles — metastable monopole-antimonopole bound states, and (3) cosmic “necklace” — a system of monopoles on strings. I also discuss the implications of the results of certain recent numerical simulations of evolution of cosmic strings in the Universe. These results, if confirmed by independent simulations, would imply that massive X-particle production and hence cosmic ray production might be a generic feature of cosmic strings, which would make cosmic strings an inevitable source of EHECR with potentially detectable flux. Indeed, in this case, we shall see that the measured EHECR flux already puts severe constraint on the energy scale of symmetry-breaking associated with any cosmic string forming phase transition in the early Universe.

I use natural units with $\hbar = c = k_B = 1$ throughout, unless otherwise stated.

Topological Defects and X Particle Production: A Brief Review

Topological Defects are sometimes characterized as “exotic”. In actual fact, TDs are routinely seen, measured, and studied in condensed matter systems in laboratories. TDs form during phase transitions associated with the phenomenon of spontaneous symmetry breaking (SSB), which is a central concept in condensed matter physics as well as in the Standard Model of particle physics. Well-known examples of TDs in condensed matter systems are vortex lines in superfluid helium, magnetic flux tubes in type-II superconductors, disclination lines and ‘hedgehogs’ in nematic liquid crystals, and so on. Perhaps what is perceived as exotic is the existence of TDs in the cosmological context. However, it has been realized for quite some time now, particularly since the early seventies, that our Universe in its early stages must have behaved very much like condensed matter systems. Indeed, ideas of unified gauge theories of elementary particle interactions taken together with the hot big-bang model of the early Universe necessarily imply that our Universe in its early history has passed through a sequence of symmetry-breaking phase transitions as it expanded and cooled through certain critical temperatures. Depending on the symmetry breaking pattern, one or more kinds of the three basic kinds of topological defects — magnetic monopoles, cosmic strings and domain walls — could be formed during some of these phase transitions[1, 2]. In fact, formation of magnetic monopoles, is *inevitable* in practically all Grand Unified Theories (GUTs) that provide a unified description of the electroweak and strong interactions³. The monopoles are analogous to the ‘hedgehogs’ in nematic liquid crystals and appear whenever the unbroken symmetry group possesses a local U(1) symmetry. The ‘global’ cosmic strings, which arise in breaking of global U(1) symmetry, are similar to vortex filaments in superfluid helium, and the ‘local’ or ‘gauge’ cosmic strings arising from breaking of a local U(1) symmetry are similar to the magnetic flux tubes in type-II superconductors. Cosmic domain walls appear whenever a discrete symmetry is spontaneously broken.

Interestingly, it has recently become possible to simulate the analogue of cosmic string formation in the early Universe by means of laboratory experiments[30] on vortex-filament formation in the superfluid transition of ³He, which occurs at a temperature of a few millikelvin. The results of these experiments have provided striking confirmation of the basic Kibble-Zurek picture[1, 2, 31] of topological defect formation in general, which was initially developed within the context of defect formation in the early Universe[1].

³The inevitability of monopole formation leads to the well-known “monopole problem” of cosmology, which historically was one of the “problems” that motivated the idea of *inflationary cosmology*; for a review, see Ref.[29]

Symmetry Breaking Phase Transitions and Formation of Topological Defects

During a symmetry breaking phase transition, the system under consideration undergoes a transition from a state of higher symmetry to one of a lower (reduced) symmetry at a critical temperature during the cooling of the system. In spontaneous symmetry breaking (SSB), the system below the critical temperature possesses multiple degenerate ground states rather than a unique ground state. These degenerate ground states differ from each other by the ‘phase angle’ or some internal degrees of freedom of the “order parameter” field (OPF) whose absolute magnitude (which is same for all the ground states) is a measure of the order (or lack of symmetry) in the system. (In particle physics, the OPF is the “higgs” field.) The symmetry under consideration is invariance of the energy (or more precisely the Lagrangian for the OPF or the higgs field) under transformations that change the ‘phase’ of the OPF. The Lagrangian is always invariant under these transformations because, by construction, it depends only on the absolute magnitude of the OPF and not on its ‘phase’. However, the ground states transform among each other under the action of these transformations, and so any chosen ground state is clearly not invariant under the transformations — the symmetry is spontaneously broken. The existence of multiple degenerate ground states is the defining characteristic of the phenomenon of spontaneous symmetry breaking. By convention, the absolute value of the OPF is taken to be zero in the high-temperature unbroken-symmetry phase and unity in the low-temperature broken symmetry phase.

Because of the availability of these multiple degenerate ground states in the low temperature phase, different parts of the system may choose to settle down to different ground states when making the transition to the low temperature phase, especially so if the transition happens in an out-of-equilibrium situation. Indeed, one expects that the choice of the phase of the OPF in regions separated by more than the correlation length of the thermal fluctuations of the OPF will be uncorrelated. The correlation length will always be finite in a finite physical system. In the context of the Universe as a whole, there is also an upper limit to the correlation length at any time t , namely, the causal horizon length $\sim ct$. Thus the choice of the phase of the OPF will be random and in general different in different parts of the Universe separated by more than the causal horizon length at the time of phase transition. This often leads to ‘obstruction’ in the way of uniform completion of the transition throughout the bulk of the system. Indeed, it is often the case that the random choice of different ground states in different regions leads to some regions being forced to remain in the unbroken symmetry phase. These regions are the ‘topological defects’.

The topological nature of the defects becomes clear when one considers the configuration of the OPF in the low temperature phase at the end of the phase transition. The choice of the ‘phase’ of the OPF corresponding to different ground states in different parts of the system may be such that, in order to avoid energetically unfavored discontinuity in the spatial variation of the OPF, the magnitude of the OPF is forced to be zero on some geometrical points, lines, or surfaces, which define the ‘center’ of the defects. Actually, a defect has a finite size dictated by the need to minimize the overall energy of the system; the absolute

value of the OPF increases *gradually* from zero at the center to its broken-symmetry-phase value at a finite distance from the center.

The topological stability of the defects is due to non-trivial topological ‘winding’ of the OPF configuration around the defect center. For example, in the case of the linear defect (the vortex filament in the superfluid helium, for example), the OPF (the wave function of the condensed helium atoms, for example) is a complex number whose phase turns by an integral multiple of 2π as one makes a complete circuit along a closed curve around any point on the defect line (the closed curve being on the normal plane cutting the defect line at the given point). Once formed, such a configuration cannot ‘unwind’ by itself and is thus topologically stable.

In the context of spontaneously broken gauge theories, explicit analytical and/or numerical finite-energy, extended, topologically stable solutions for the higgs- and gauge field configurations representing cosmic strings, monopoles and domain walls are known; see Ref.[2] for review. In the broken-symmetry phase, a higgs field responsible for spontaneous symmetry breaking of a local gauge theory is massive, as are the gauge bosons of the theory, the mass scale being set by the absolute magnitude of the higgs field (more precisely, its vacuum expectation value) in the broken symmetry phase. The size of the ‘core’ of a defect is of order m_X^{-1} , where X represents the higgs or the gauge field. Within the core, the symmetry remains unbroken, and the energy density (associated with the higgs and the gauge fields) is higher within the core than outside. The topological stability of the defect ensures the ‘trapping’ of the excess energy within the core of the defect, which is what makes a defect massive. It can be shown that the mass scale of a defect is fixed by the energy (or temperature) scale of the symmetry breaking phase transition at which the defect is formed. Thus, if we denote by T_c the critical temperature of the defect-forming phase transition in the early Universe, then the mass of a monopole formed at that phase transition is roughly of order T_c , the mass per unit length of a cosmic string is of order T_c^2 , and the mass per unit area of a domain wall is of order T_c^3 .

The X particles are the quanta of excitations of the higgs and gauge fields. In the broken symmetry phase, these quanta are massive, their mass is also roughly of order T_c . These massive quanta typically have very short life times, and so they all decayed away quickly soon after the phase transition in the early Universe, and none of those X particles survive in the present Universe. This is to say that outside of a defect in the low-energy Universe today, the higgs and the gauge fields are in their ground states and no excitations of the X particle quanta are present. However, inside the core of a defect, the symmetry is unbroken — the X particles are massless inside. Topological stability of the defect prevents this “piece of the early Universe” trapped inside the defect from decaying. If, however, there is a process which removes this topological protection, then the energy trapped inside the defect will dissociate into quanta of the X particles which, being now in the broken-symmetry phase, will be massive and short lived, decaying into elementary particles such as quarks and leptons which, in turn, would eventually materialize into energetic nucleons, photons, neutrinos, etc., that might contribute to the observed EHECR flux.

Production of X particles from TDs may happen in a variety of ways directly or indi-

rectly related to local removal of topological stability of (parts of) TDs. Examples include ‘cusp’ evaporation from cosmic strings[6], collapse of macroscopic cosmic string loops[8], shrinking of cosmic string loops to radii of order m_X^{-1} [9], annihilation of a monopole with an antimonopole[4, 10], and so on. In the case of current-carrying superconducting cosmic strings[32, 5], the charge carriers (which could be quanta of a superheavy fermion field trapped in ‘zero mode’ inside the string, or a charged scalar field living inside the string due to energetic reasons) are expelled from the string when the current on the string reaches a critical value — in the vacuum away from the string, these charge carriers act as the massive X particles. In the case of ‘ordinary’ cosmic strings, recent field theory simulations [33] of evolution of cosmic strings in the early Universe show that a cosmic string network loses energy directly into oscillations of the underlying gauge and higgs fields ‘constituting’ the string, which in quantum theory, correspond to quanta of massive X particles — a result which has important implications for both cosmic strings as well as for EHECR; this result, however, remains to be confirmed by independent simulations.

X-Particle Production Rate

The number density of X particles produced by TDs per unit time, dn_X/dt , can be generally written as[3]

$$\frac{dn_X}{dt}(t) = \frac{Q_0}{m_X} \left(\frac{t}{t_0}\right)^{-4+p}, \quad (1)$$

where t_0 denotes the present epoch, and Q_0 is the rate of energy density injected in the form of X particles in the present epoch. The quantity Q_0 and the parameter p depend on the specific TD process under consideration. In writing Eq. (1) it is assumed that the only time scale in the problem is the hubble time t and that any other time scale involved can be expressed in terms of the hubble time. Similarly, we assume that any energy scale involved in the problem is expressible in terms of the energy scale η of the symmetry breaking at which the TDs under consideration are formed. (Note that m_X is fixed by η .) These assumptions are sometimes expressed by saying that the TDs under consideration evolve in a scale independent way. Indeed, it turns out that Eq. (1) is a phenomenologically good parametrization for the specific TD processes studied so far. For example, $p = 1$ for a process of X particle production from cosmic string loops [8], for a process involving collapsing monopole-antimonopole bound states [4, 10], for a process of particle production from monopole-string systems called “necklaces” [11], and so on, while $p = 0$ for a process involving superconducting cosmic string loops [5].

Note that X particle production from TDs may occur continually at all epochs after the formation of the relevant TDs in the early Universe. However, only those X particles produced in the relatively recent epochs and at relatively close-by, non-cosmological distances ($\lesssim 100$ Mpc) are relevant for the question of EHECR. This is because, nucleons of energies above 10^{11} GeV produced by the decay of X particles occurring at distances much larger than ~ 50 Mpc suffer drastic energy loss during their propagation, due to photopion production on the the cosmic microwave background radiation (CMBR) fields (the so-called “GZK

effect” [34]), and hence do not survive as EHECR particles today. Distance of sources of photons of energies above $\sim 10^{11}$ GeV are also similarly restricted due to absorption through e^+e^- production on the radio background photons (see, e.g., [26]). The neutrinos, however, can survive from much earlier cosmological epochs, and may, if detected, prove to be the ultimate discriminant between a TD scenario and a more conventional scenario of origin of EHECR.

From X Particles to ‘Observable’ Particles

The X particles released from TDs would decay typically into quarks and leptons. The life-time τ is typically $\sim (\alpha m_X)^{-1}$ (where $\alpha \sim \text{few} \times 10^{-2}$), which for $m_X \sim 10^{16}$ GeV is $\sim 10^{-39}$ sec or so. The decay is, therefore, essentially instantaneous at late cosmological epochs of interest to us. The quarks would hadronize (typically on a strong interaction time scale $\sim 10^{-23}$ sec, i.e., again practically instantaneously) by producing jets of hadrons, most of which would eventually be light mesons (pions) with a small admixture (typically $\lesssim 10\%$) of baryons and antibaryons (nucleons and antinucleons). The neutral pions decay to two photons, while the decay of charged pions gives rise to neutrinos. Some leptons (charged as well as neutral) could also be produced directly from the X particle decay. But by far the largest number of nucleons, photons, and neutrinos, would be produced through the hadronic channel. The spectra of produced particles are, therefore, essentially determined by the process of fragmentation of quarks/gluons into hadrons as described by QCD.

Quark \rightarrow Hadron Fragmentation Spectrum

The exact process by which a single high energy quark gives rise to a jet of hadrons is not known; it involves some kind of non-perturbative physics that is not well understood. However, different semi-phenomenological approaches have been developed which describe the hadronic “fragmentation spectrum” of quarks/gluons that are in good agreement with the currently available experimental data on inclusive hadron spectra in quark/gluon jets in a variety of high energy processes.

In these approaches, the process of production of a jet containing a large number of hadrons, by a single high energy quark (or gluon), is ‘factorized’ into two stages. The first stage involves ‘hard’ processes involving large momentum transfers, whereby the initial high energy quark emits ‘bremsstrahlung’ gluons which themselves create more quarks and gluons through various QCD processes. These hard processes are well described by perturbative QCD. Thus a single high energy quark gives rise to a ‘parton cascade’ — a shower of quarks and gluons — which, due to the high energy nature of the process, is confined in a narrow cone or jet whose axis lies along the direction of propagation of the original quark. This first stage of the process, i.e., the parton cascade development, described by perturbative QCD, is terminated at a cut-off value, $\langle k_{\perp}^2 \rangle_{\text{cut-off}}^{1/2} \sim 1$ GeV, of the typical transverse momentum. Thereafter, the second stage, involving the non-perturbative “confinement” process, takes over binding the quarks and gluons into color neutral hadrons. This second stage is usually

described by one of the available phenomenological hadronization models such as the LUND string fragmentation model [35] or the cluster fragmentation model [36]. Detailed Monte Carlo numerical codes now exist [36, 37, 38] which incorporate the two stages outlined above. These codes provide a reasonably good description of a variety of relevant experimental data. Clearly, however, this is a numerically intensive approach.

Local Parton-Hadron Duality

There is an alternative approach that is essentially analytical and has proved very fruitful in terms of its ability to describe the gross features of hadronic jet systems, such as the inclusive spectra of particles, the particle multiplicities and their correlations, etc., reasonably well. This approach is based on the concept of ‘‘Local Parton Hadron Duality’’ (LPHD) [39]. Basically, in this approach, the second stage involving the non-perturbative hadronization process mentioned above is ignored, and the hadron spectrum is taken to be the same, up to an overall normalization constant, as the spectrum of partons (i.e., quarks and gluons) in the parton cascade after evolving the latter all the way down to a cut-off transverse momentum $\langle k_{\perp}^2 \rangle_{\text{cut-off}}^{1/2} \sim R^{-1} \sim \text{few hundred MeV}$, where R is a typical hadronic size. At present the only justification for such an approach seems to be that it gives a remarkably good description of the experimental data including recent experimental results from LEP, HERA and TEVATRON [40]. Justification of LPHD at a more fundamental theoretical level, however, is not yet available. Nevertheless, it serves as a good phenomenological tool.

The main assumption in LPHD is that the actual hadronization process, i.e., the conversion of the quarks and gluons in the parton cascade into color neutral hadrons, occurs at a low virtuality scale of order of a typical hadron mass independently of the energy of the cascade initiating primary quark, and involves only low momentum transfers and local color ‘re-arrangement’ which somehow does not drastically alter the form of the momentum spectrum of the particles in the parton cascade already determined by the ‘hard’ (i.e., large momentum transfer) perturbative QCD processes. Thus, the non-perturbative hadronization effects are lumped together in an ‘unimportant’ overall normalization constant which can be determined phenomenologically.

A good quantitative description of the perturbative QCD stage of the parton cascade evolution is provided by the so-called Modified Leading Logarithmic Approximation (MLLA) [41] of QCD, which allows the parton energy spectrum to be expressed analytically in terms of functions depending on two free parameters, namely, the effective QCD scale Λ_{eff} (which fixes the effective running QCD coupling strength $\alpha_s^{\text{eff}}(\tilde{Q}^2)$) and the transverse momentum cut-off \tilde{Q}_0 . For the case $\tilde{Q}_0 = \Lambda_{\text{eff}}$, the analytical result simplifies considerably, and one gets what is referred to as the ‘‘limiting spectrum’’ [39, 40]. For asymptotically high energies of interest, i.e., for energies E_{jet} of the original jet-initiating quark satisfying $E_{\text{jet}} \gg \Lambda_{\text{eff}}$, the limiting spectrum can be approximated by a Gaussian in the variable $\xi \equiv \ln(1/x)$, with $x \equiv E_{\text{parton}}/E_{\text{jet}}$, E_{parton} being the energy of a quark (parton) in the jet:

$$x \frac{dN_{\text{parton}}(Y, x)}{dx} \approx \frac{N_{\text{parton}}(Y)}{\sigma \sqrt{2\pi}} \exp \left[-\frac{(\xi - \bar{\xi})^2}{2\sigma^2} \right], \quad (2)$$

where $Y \equiv \ln(E_{\text{jet}}/\Lambda_{\text{eff}})$, $\bar{\xi} \approx Y/2$, $2\sigma^2 = \left(\frac{bY^3}{36N_c}\right)^{1/2}$ with $b \equiv (11N_c - 2N_f)/3$, N_c being the number of colors and N_f the number of flavors of quarks involved, and $N_{\text{parton}}(Y) \sim \exp\{(16N_c Y/b)^{1/2}\}$ is the average total multiplicity of the partons in the jet.

Eq. (2) gives us the spectrum of the partons in the jet. By LPHD hypothesis, the shape of the hadron spectrum, dN_h/dx (with $x = E_h/E_{\text{jet}}$, E_h being the energy of a hadron in the jet), is given by the same form as in Eq. (2), except for an overall normalization constant that takes account of the effect of conversion of partons into hadrons. Phenomenologically, for given values of Λ_{eff} and E_{jet} , the normalization constant can be determined simply from overall energy conservation, i.e., from the condition $\int_0^1 x \frac{dN_h(Y,x)}{dx} dx = 1$. The value of Λ_{eff} is not known *a priori*, but a fit to the inclusive charged particle spectrum in e^+e^- collisions at center-of-mass energy $E_{\text{cm}} = 2E_{\text{jet}} \sim 90$ GeV (Z-resonance) gives $\Lambda_{\text{eff}}^{\text{ch}} \sim 250$ MeV.

Note that, within the LPHD picture, there is no way of distinguishing between various different species of hadrons. Phenomenologically, the experimental data can be fitted by using different values of Λ_{eff} for different species of particles depending on their masses. For our consideration of particles at EHECR energies, all particles under consideration will be extremely relativistic, and since, in our case, $E_{\text{jet}} \sim m_X/2 \gg \Lambda_{\text{eff}}$, the hadron spectrum will be relatively insensitive to the exact value of Λ_{eff} . Also, one can safely assume that at the asymptotically high energies of our interest, all hadrons — mesons as well as baryons — will have the same spectrum. However, the dominant species of particles in terms of their overall number will be the light mesons (pions); baryons typically constitute a fraction of $\lesssim (3 - 10)\%$ as indicated by existing collider data. For more details on various phenomenological aspects of the LPHD hypothesis, see the reviews [40].

Nucleon, Photon and Neutrino Injection Spectra

Using the MLLA + LPHD hadron spectrum discussed above, and assuming that each X particle on average undergoes N -body decay (typically $N \leq 3$) to N_q quarks (including antiquarks) and N_ℓ leptons (neutrinos and/or charged leptons), so that $N = N_q + N_\ell$, and assuming that the energy m_X is shared roughly equally by the N primary decay products of the X , the nucleon injection spectrum, $\Phi_N(E_i, t_i)$, from the decay of all X particles from TDs at any time t_i can be written as

$$\Phi_N(E_i, t_i) = \frac{dn_X(t_i)}{dt_i} N_q f_N \frac{1}{E_i} N_{\text{norm}} \frac{1}{\sigma\sqrt{2\pi}} \exp\left[-\ln^2\left(\frac{x_*}{x}\right)\right], \quad (3)$$

where E_i denotes the energy at injection, $\frac{dn_X}{dt_i}$ is the number of X particle released per unit volume per unit time at time t_i , f_N is the nucleon fraction in the hadronic jet produced by a single quark, $x = NE_i/m_X$, $x_* = (N\Lambda_{\text{eff}}/m_X)^{1/2}$, and N_{norm} is the normalization constant defined by

$$N_{\text{norm}}(m_X) = \left(\int_0^1 dx \frac{1}{\sigma\sqrt{2\pi}} \exp\left[-\ln^2\left(\frac{x_*}{x}\right)\right]\right)^{-1}. \quad (4)$$

An important point about the nucleon injection spectrum given by Eq. (3) is that, unlike the spectrum predicted in the standard diffusive shock acceleration theory (see, e.g.,

Refs. [20, 18, 19]), the injection spectrum in the TD scenario (or, for that matter, in any non-acceleration scenario in which the energetic particles arise from decay of massive elementary particles), is not, in general, a power-law in energy. Although, in the energy regions of our interest, the spectrum (3) can be approximated [7] by power-law segments ($\propto E_i^{-\alpha}$), the power-law index α , in the energy regions of interest, is generally smaller than that in shock acceleration theories — the latter typically predict $\alpha \geq 2$. In other words, the injection spectrum in non-acceleration theories is generally harder (or flatter) compared to that in conventional acceleration theories. This fact has important consequences; it leads to the prediction of a pronounced “recovery” [3] of the evolved nucleon spectrum after a partial GZK “cut-off” and the consequent flattening of the spectrum above $\sim 10^{11}$ GeV. A relatively hard spectrum may also naturally give rise to a “gap” in the measured EHECR spectrum [14].

The photon injection spectrum from the decay of the neutral pions ($\pi^0 \rightarrow 2\gamma$) in the jets is given by

$$\Phi_\gamma(E_i, t_i) \simeq 2 \int_{E_i}^{m_X/N} \frac{dE}{E} \Phi_{\pi^0}(E), \quad (5)$$

where $\Phi_{\pi^0} \simeq \frac{1}{3} \frac{1-f_N}{f_N} \Phi_N$ is the neutral pion spectrum in the jet.

Similarly, the neutrino ($\nu_\mu + \bar{\nu}_\mu$) injection spectrum resulting from the charged pion decay [$\pi^\pm \rightarrow \mu^\pm \nu_\mu(\bar{\nu}_\mu)$] can be written as [42, 3]

$$\Phi(\nu_\mu + \bar{\nu}_\mu)(E_i) \simeq 2.34 \int_{2.34E_i}^{m_X/N} \frac{dE}{E} \Phi_{(\pi^++\pi^-)}(E), \quad (6)$$

where $\Phi_{(\pi^++\pi^-)} \simeq \frac{2}{3} \frac{1-f_N}{f_N} \Phi_N$.

The decay of each muon (from the decay of a charged pion) produces two more neutrinos and an electron (or positron): $\mu^\pm \rightarrow e^\pm \nu_e(\bar{\nu}_e) \bar{\nu}_\mu(\nu_\mu)$. Thus each charged pion eventually gives rise to three neutrinos: one ν_μ , one $\bar{\nu}_\mu$ and one ν_e (or $\bar{\nu}_e$), all of roughly the same energy. So the total $\nu_\mu + \bar{\nu}_\mu$ injection spectrum will be roughly twice the spectrum given in Eq. (6), while the total $\nu_e + \bar{\nu}_e$ spectrum will be roughly same as that in Eq. (6).

Note that, if the hadron spectrum in the jet is generally approximated by a power-law in energy, then nucleon, photon and neutrino injection spectra will also have the same power-law form all with the same power-law index.

It is worth emphasizing here that while using the LPHD hadron spectrum in the analysis of the TD scenario of EHECR one should keep in mind that there is a great deal of uncertainty involved in extrapolating the QCD based hadron spectra — which have been tested so far only at relatively ‘low’ energies of ~ 100 GeV — to the extremely high energies of $\sim 10^{15}$ GeV or so.

Evolution of the Particle Spectra

Nucleons

The evolution of the nucleon spectrum is mainly governed by interactions of the nucleons with the CMBR. The relevant interactions are pair production by protons ($p\gamma_b \rightarrow pe^+e^-$),

photoproduction of single or multiple pions by nucleons N ($N\gamma_b \rightarrow Nn\pi, n \geq 1$), and neutron decay. Here γ_b stands for a background photon, in this case, a CMBR photon. At EHECR energies, the photopion production is the dominant process. This is a drastic energy loss process for nucleons, and is the basis of the well-known prediction of the GZK cut-off [34] of the evolved EHECR nucleon spectrum at energies above $\sim 10^{11}$ GeV. This process also limits the distance of a possible source of the observed EHECR particles to distances less than ~ 50 Mpc [34, 13, 22].

γ -rays

The γ -rays at EHECR energies interact via pair production (PP: $\gamma\gamma_b \rightarrow e^+e^-$) and double pair production (DPP: $\gamma\gamma_b \rightarrow e^+e^-e^+e^-$), while the electrons (positrons) interact via inverse Compton scattering (ICS: $e\gamma_b \rightarrow e'\gamma$) and triplet pair production (TPP: $e\gamma_b \rightarrow ee^+e^-$). In addition, the electrons (positrons) suffer synchrotron energy loss in the extragalactic magnetic field (EGMF). The background photons (γ_b) involved in the PP process are mainly the universal radio background (URB) photons for γ -rays above $\sim 10^{19}$ eV, the CMBR photons for γ -rays between $\sim 10^{14}$ eV and $\sim 10^{19}$ eV, and the infrared and optical (IR/O) background photons for γ -rays below $\sim 10^{14}$ eV.

The evolution of the γ -ray spectrum is complicated due to the fact that PP and ICS processes together lead to development of electromagnetic (EM) cascades, whereby any electromagnetic energy in the form of γ -rays and/or electrons (positrons) released at an energy which is above the threshold for PP process on photons of a particular background, cascades down to progressively lower energies through a cycle of PP interactions (on the photons of progressively higher energy backgrounds) and ICS interactions (mainly on the CMBR). The cascading has the overall effect of increasing the γ -ray flux at EHECR energies because it causes an effective increase of the attenuation length of these γ -rays. Further cascading by any cascade photon stops either if the remaining path length of the cascade photon, as it propagates from its point of creation to the observation point, becomes less than the mean free path for the PP process on the relevant background photons, or if the energy of the propagating cascade photon falls below the threshold for the PP process. Thus, depending on the distance at which they are first injected, γ -rays of EHECR energies can, after propagation, give rise to a γ -ray spectrum that may span the energy range from (say) a few tens of MeV all the way up to EHECR energies. This, of course, means that any model of electromagnetic energy injection at EHECR energies has to meet the constraint that the resulting cascade γ -ray flux at lower energies should not exceed the measured flux at those energies. In the context of TD models of EHECR, this was first pointed out in Ref. [28].

The mean attenuation length of EHE γ -rays depends strongly on the density of URB and on the strength of the EGMF, both of which are uncertain at the present time. The EGMF typically inhibits cascade development because of synchrotron cooling of the e^-e^+ pairs produced in the PP process. Depending on the strength of the EGMF, the synchrotron cooling time scale may be shorter than the time scale of ICS, in which case the e^- or the e^+ under consideration loses energy through synchrotron radiation before it can undergo ICS,

and thus cascade development stops. In this case the γ -ray flux is determined mainly by the “direct” γ -rays, i.e., the ones that originate at distances less than the absorption length due to PP process. The energy lost by synchrotron cooling does not, however, disappear — rather, it appears at a lower energy and can initiate fresh EM cascades by interacting with the photons of a higher energy background such as CMBR or IR/O depending on its energy. So the overall effect of a relatively strong EGMF is to deplete the γ -ray flux above some energy in the EHE region and increase the γ -ray flux below a corresponding energy in the ‘low’ (MeV – GeV) energy region, where it will have to meet the constraints imposed by the measured extragalactic diffuse γ -ray background [43, 44].

In addition to uncertainties in the strength of EGMF and the URB, another major source of uncertainty in the cascade calculation is the poorly known IR/O background (see, e.g., Ref. [45] for a recent discussion of IR/O backgrounds). The latter strongly influences the cascade spectrum in the energy range from $\sim 10^{11}$ eV to $\sim 10^{14}$ eV. Below this range, however, the cascade spectrum becomes relatively insensitive [46] to the model parameters that determine the IR/O background. This is a fortunate circumstance because this implies that the constraints on TD models derived [15, 16, 17, 46] by comparing the measured 100 MeV – 10 GeV γ -ray background with TD model predictions are relatively insensitive to uncertainties in our precise knowledge of the IR/O background, and hence are fairly robust.

Neutrinos

EHE neutrinos suffer absorption through fermion-antifermion pair production on the thermal background neutrinos ($\nu + \bar{\nu}_b \rightarrow f\bar{f}$), where $f \equiv e, \mu, \tau, \nu, q$, and ν_b is a thermal background neutrino. Due to this absorption process, neutrinos of present observed energy $E_{\nu,0}$ would have to have been injected at redshifts less than $z_a(E_{\nu,0}) \simeq 3.5 \times 10^2 (10^{20} \text{ eV}/E_{\nu,0})^{2/7}$, for $E_{\nu,0} \gtrsim 3 \times 10^{14}$ eV [3].

Actually, the μ ’s, τ ’s, and quarks created in the above absorption process generate further neutrinos through decay of the μ ’s and τ ’s and through decay of the charged pions created by quark fragmentation. This leads to a “neutrino cascade” [27], effectively increasing the size of the “neutrino horizon” of the Universe. This, in turn, has the effect of increasing the overall neutrino flux around 10^{20} eV by a factor of few relative to the case when the cascading effect is not taken into account.

Recently, it has been pointed out [47] that if neutrinos have a small mass m_ν in the eV range, then EHE neutrinos (antineutrinos) of energy $\sim 4 (eV/m_\nu) \times 10^{12}$ GeV will annihilate on the relic antineutrinos (neutrinos) to produce the Z-boson with a resonant cross section of $\sim 10^{-32}$ cm². The hadronic decay of the Z will produce additional photons, neutrinos and nucleons, which will add to the photon and neutrino cascading processes mentioned above. This process may also leave specific signatures on the EHE neutrino spectrum, the detection of which may in the end provide an indirect signature of the neutrino mass and hence of dark matter. Detailed self-consistent calculation of nucleon, photon and neutrino fluxes, however, remain to be done.

Predicted Particle Fluxes and Constraints on TD models

As discussed above, the predicted particle fluxes depend on a number of parameters: the X particle mass m_X , the strength of EGMF, the URB, the injection spectra, and so on. Recently, detailed numerical calculation of the particle spectra, especially the spectrum of γ -rays in the entire energy range from $\sim 10^8$ eV to $\sim 10^{25}$ eV, have been done [15, 16, 17] taking into account the effects of electromagnetic cascading and EGMF. Fig. 1 shows the predicted

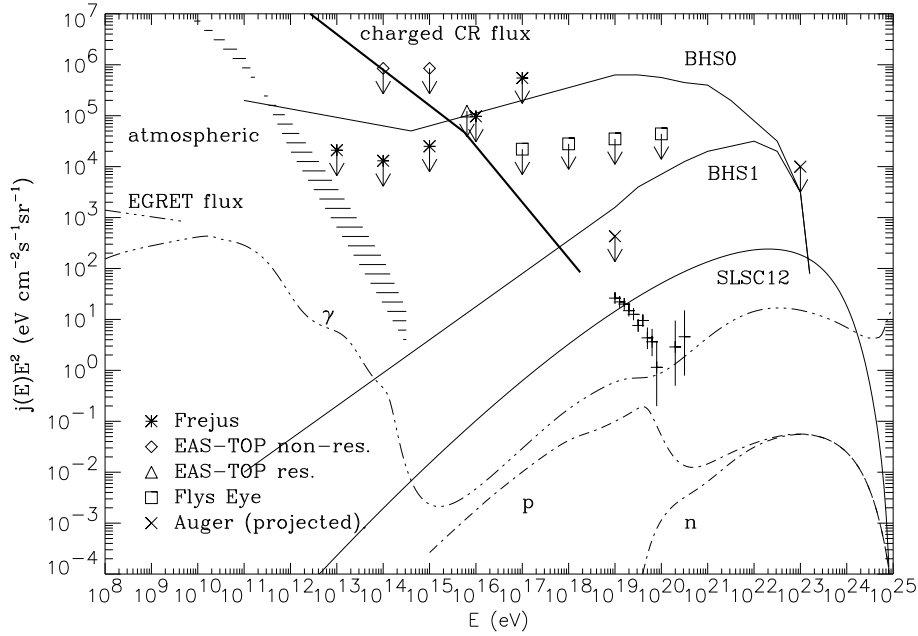


Figure 1: Predicted fluxes of γ -rays (dash - triple dotted line), protons and neutrons (dash-dotted lines) and $(\nu_\mu + \bar{\nu}_\mu)$ (solid lines) for TD models with $p = 1$, $m_X = 10^{16}$ GeV and EGMF of 10^{-12} Gauss. The neutrino curve marked “SLSC12” corresponds to the calculation of Ref. [16], while the curves marked “BHS0” and “BHS1” represent the neutrino fluxes from Ref. [3] and correspond respectively to $p = 0$ and the $p = 1$ models. Also shown are the estimates of the atmospheric neutrino background for different zenith angles [48] (hatched region marked “atmospheric”). Data points with error bars represent the combined cosmic ray data from the Fly’s Eye and AGASA experiments [12] above 10^{19} eV, and the thick solid line represents piecewise power-law fit to the observed charged CR flux. The dash - triple dotted line on the left margin represents experimental upper limits on the diffuse γ -ray flux at 100 MeV – 5 GeV from EGRET data [43, 44]. Points with arrows pointing downwards represent approximate upper limits on the diffuse neutrino flux from Frejus [49], the EAS-TOP [50], and the Fly’s Eye [51] experiments, as indicated. The projected limit shown for the proposed Auger experiment assumes the acceptance estimated in Ref. [52] for non-detection over a five year period. (Courtesy G. Sigl)

diffuse particle fluxes for a representative set of values of various parameters involved. Here I discuss only the predicted diffuse fluxes of particles assuming uniform distribution of TD sources in the Universe. (Possible individual “bursting” sources of EHECR and the possible reconstruction of their “images” from data on arrival direction, arrival time and energy associated with individual events, leading to information about the source characteristics and, in particular about the EGMF, are discussed in the talk by G. Sigl; see this volume.)

Because the magnitude of X particle production rate is not known *a priori*, the best one can do at the present time is adopt a suitable normalization procedure for the absolute flux so as to be able to explain the EHECR data, and then check whether this normalization is consistent with all relevant observational data, not just on EHECR particles, but also on other relevant particle fluxes at lower energies, especially the diffuse gamma ray background measurements in the MeV – GeV region. The normalization of the absolute fluxes in Fig. 1 is optimized in the sense that it has been determined by fitting the ‘observable’ particle (i.e., the combined nucleon and γ -ray) fluxes to the measured EHECR data by the maximum likelihood method [14] and corresponds to a likelihood significance of $> 50\%$.

It is clear that TD models, while potentially contributing dominantly to the particle fluxes above $\sim 10^{20}$ eV, make negligible contribution to cosmic ray flux below $\sim 10^{19}$ eV because of the relatively hard nature of the particle spectra in these models. Thus the flux below $\sim 2 \times 10^{19}$ eV is presumably due to a conventional acceleration scenario, and was not included in the fitting procedure.

Since pions are the most numerous particles in the jets, their decay products, i.e., photons and neutrinos dominate the number of particles at production. Since neutrinos suffer little attenuation and can come to us unattenuated from large cosmological distances (except for absorption due to e^+e^- pair production by interacting with the cosmic thermal neutrino background, the path length for which is $\gg 100$ Mpc), their fluxes, as expected, are the largest among all particles at the highest energies. However, their detection probability is much lower compared to those for protons and photons⁴. Photons also far outnumber nucleons at production, and depending on the level of the URB and EGMF, may dominate over the nucleon flux and thus dominate the ‘observable’ particle flux at EHECR energies.

An important point to note is that photons and neutrinos in the TD scenario are *primary* particles in that they are produced directly from the decay of the pions in the hadronic jets. In contrast, photons and neutrinos in conventional acceleration scenarios can be produced only through *secondary* processes — they are mainly produced by the decay of photoproduced pions resulting from the GZK interactions of primary HECR nucleons (produced by the acceleration process) with CMBR photons [42]. Of course, these secondary neutrinos and photons would also be there in the TD scenario, but their fluxes are sub-dominant to the primary ones at the highest energies.

The *shapes* of the EHE nucleon- and γ -ray spectra In the TD scenario are “universal” [3, 26] in the sense that they are independent of specific TD process even though different

⁴The EHE neutrinos of TD origin would, however, be potentially detectable by the proposed space-based detectors like OWL and AIRWATCH, and ground based detectors like Auger, Telescope Array, and so on; see articles on these detector projects in this volume.

TD sources evolve differently (as parametrized by the parameter p in the X particle production rate). This is because, at these energies, the attenuation lengths of nucleons and γ -rays are small ($\lesssim 100$ Mpc) compared to Hubble length and so the effects of unknown cosmological evolution of the TD sources are negligible compared to propagation effects. The universal shapes of the EHECR nucleon and γ -ray spectra reflect their injection spectra, which, as discussed earlier, are determined by QCD. Thus, large statistics measurement of the EHECR spectrum by future detectors may give us a probe of new physics, and in particular QCD, at energies not currently accessible in laboratory accelerators, *provided* a TD-like non-acceleration scenario of origin of EHECR is correct.

In contrast to the EHECR nucleons and γ -rays, the predicted γ -ray flux below $\sim 10^{14}$ eV (the threshold for pair production on the photons of CMBR) and the predicted EHE neutrino flux depend on the total energy released integrated over redshift and hence are dependent on the specific TD model (i.e., specific value of p). In particular, the γ -ray flux below $\sim 10^{11}$ eV scales as the total electromagnetic energy released from X particles integrated over all redshifts and increases with decreasing value of p . This has been used to constrain [53] TD models from considerations of CMBR distortions and from independent considerations of modified light element abundances due to ^4He photodisintegration; for example, this rules out [53] the $p = 0$ TD model.

The γ -ray flux in Fig. 1 is consistent with the estimates of the upper limit on the background in the 100 MeV to ~ 5 GeV from EGRET data [43]. Very recently, new estimates of the background flux have been presented [44] which now extend up to ~ 100 GeV with roughly the same power-law index as the earlier estimates [43]. If the EGMF is significantly larger than the value assumed ($\sim 10^{-12}$ Gauss) for the calculation of Fig. 1, then the electromagnetic cascade energy transferred to the relevant low energy region will be higher, and in this case the γ -ray flux in Fig. 1 will only be marginally consistent, or may even be inconsistent, with the experimental diffuse background flux estimates. Note, however, that the fluxes in Fig. 1 correspond to the case $m_X = 10^{16}$ GeV. Lower values of m_X are possible, which will give lower contribution to the low energy diffuse flux while at the same time producing enough energy in the form of X particles to explain the observed EHECR flux. This can be seen as follows:

As we shall discuss in more details in the next section, for a relatively hard power-law photon injection spectrum $\propto E^{-\alpha}$ with $\alpha < 2$, the energy injection rate Q_0 required to match a given differential EHECR flux at a given energy decreases with decreasing value of m_X (provided, of course, $m_X > 10^{11}$ GeV, the energy of the highest energy event). For example, it is easy to see (see next section) that for a photon injection spectrum $\propto E^{-1.5}$, the value of Q_0 required to explain the EHECR flux is roughly proportional to $m_X^{1/2}$. And since the cascade γ -ray flux in the $\lesssim 100$ GeV region is essentially directly proportional to Q_0 injected at EHECR energies, a reduction by a factor of 10, for example, of the predicted γ -ray flux in the $\lesssim 100$ GeV region is easily achieved by reducing m_X by about two orders of magnitude, i.e., for $m_X \lesssim 10^{14}$ GeV. And, of course, as already mentioned, the low energy γ -ray flux is also reduced if the EGMF strength is lower.

Thus, it seems that TD models of EHECR with $m_X \sim 10^{16}$ GeV and/or high EGMF

($\sim 10^{-9}$ Gauss) are somewhat difficult to simultaneously reconcile with EHECR data and the low energy diffuse γ -ray background. On the other hand, models with $m_X \lesssim 10^{14}$ GeV and low EGMF ($\lesssim 10^{-11}$ Gauss) can explain the EHECR data and at the same time be consistent with all existing data.

The neutrino flux indicated by curve marked “SLSC12” in Figure 1 corresponds to overall X particle production rate obtained by the maximum likelihood normalization of the ‘observable’ (i.e., photon plus nucleon) flux to the EHECR data for the $p = 1$ TD model. The *predicted* level of the neutrino flux, therefore, depends on the value of EGMF, the radio background, etc., which go into determining the photon flux. The earlier flux estimate (the curve marked “BHS1”) in Fig.1 is higher simply because the overall X particle production rate was normalized to a higher value; that normalization was obtained by normalizing the predicted *proton* (as opposed to photon) flux with the measured flux at a lower energy $\sim 5 \times 10^{19}$ eV (where the measured cosmic ray flux is higher than that at EHECR energies) — the Fly’s Eye and AGASA highest energy events beyond 10^{20} eV [12] were not yet discovered at that time! The $p = 0$ model is ruled out by the upper limits from Frejus as well as EAS-TOP experiments. (Actually, the $p = 0$ model is also ruled out from considerations [53] of ${}^4\text{He}$ photo-disintegration and CMBR distortions as mentioned above — it corresponds to unacceptably high rate of energy injection in the early cosmological epochs.) On the other hand, the new neutrino flux estimates for the $p = 1$ model are consistent with all existing experimental upper limits. At energies $\gtrsim 10^{20}$ eV, the predicted neutrino flux in the $p = 1$ TD model also dominates over the predicted flux from blazars/AGNs as well as over the predicted flux of “cosmogenic” neutrinos produced by interactions of UHE cosmic rays with CMBR [54] (not shown in Fig. 1). For more details on the detectability of neutrino fluxes in TD models, see, e.g., Ref. [16, 27, 55, 56].

X-Particle Production Rate Required to Explain the EHECR Flux: A Benchmark Calculation

To have an idea of the kind of numbers for the required X particle production rate, we can perform a simple (albeit crude) benchmark calculation as follows:

Since in TD models, photons are expected to dominate the observable EHECR flux, let us assume for simplicity that the highest energy events are due to photons. Let us assume a typical three-body decay mode of the X into a $q\bar{q}$ pair and a lepton: $X \rightarrow q\bar{q}\ell$. The two quarks will produce two hadronic jets. Let f_π denote the total pion fraction in a jet. Then the photons from the two jets carry a total energy $E_{\gamma,\text{Total}} \simeq \left(\frac{2}{3} \times 0.9 \times \frac{1}{3}\right) m_X (f_\pi/0.9) = 0.2m_X(f_\pi/0.9)$. Let us assume a power-law hadronic fragmentation spectrum with index 1.5. Then the photon injection spectrum from a single X particle can be written as

$$\frac{dN_\gamma}{dE_\gamma} = \frac{3}{m_X} \times 0.3 \left(\frac{3E_\gamma}{m_X}\right)^{-1.5} \left(\frac{f_\pi}{0.9}\right), \quad (7)$$

which is properly normalized with the total photon energy $E_{\gamma,\text{Total}}$. We shall neglect cosmo-

logical evolution effects since photons of EHECR energies have a cosmologically negligible path length of only \sim few tens of Mpc for absorption through pair production on the radio background.

With these assumptions, the photon flux $j_\gamma(E_\gamma)$ at the observed energy E_γ is simply given by

$$j_\gamma(E_\gamma) \simeq \frac{1}{4\pi} \lambda(E_\gamma) \frac{dn_X}{dt} \frac{dN_\gamma}{dE_\gamma}, \quad (8)$$

where $\lambda(E_\gamma)$ is the pair production absorption path length of a photon of energy E_γ .

Noting that $dn_X/dt = Q_0/m_X$, and normalizing the above flux to the measured EHECR flux corresponding to the highest energy event at $\sim 3 \times 10^{20}$ eV, given by $j(3 \times 10^{20} \text{ eV}) \approx 5.6 \times 10^{-41} \text{ cm}^{-2} \text{ eV}^{-1} \text{ sec}^{-1} \text{ sr}^{-1}$, we get

$$Q_{0,\text{required}} \approx 2.1 \times 10^{-21} \text{ eV cm}^{-3} \text{ sec}^{-1} \left(\frac{10 \text{ Mpc}}{\lambda_{\gamma,300}} \right) \left(\frac{m_X}{10^{16} \text{ GeV}} \right)^{1/2}, \quad (9)$$

or

$$\left(\frac{dn_X}{dt} \right)_{0,\text{required}} \approx 2.1 \times 10^{-46} \text{ cm}^{-3} \text{ sec}^{-1} \left(\frac{10 \text{ Mpc}}{\lambda_{\gamma,300}} \right) \left(\frac{m_X}{10^{16} \text{ GeV}} \right)^{-1/2}, \quad (10)$$

where $\lambda_{\gamma,300}$ is the absorption path length of a 300 EeV photon ($1 \text{ EeV} \equiv 10^{18} \text{ eV}$). The subscript 0 stands for the present epoch.

The above numbers are probably uncertain by up to an order of magnitude depending on the exact form of the injection spectrum, the absorption path length of EHECR photons, electromagnetic cascading effect, and so on. Indeed, since electromagnetic cascading effect (which we have neglected here) generally increases the photon flux, the above numbers are most likely overestimates. Nevertheless, they do serve as crude benchmark numbers. These numbers indicate that in order for TDs to explain the EHECR events, the X particles must be produced in the present epoch at a rate of $\sim 2 \times 10^{35} \text{ Mpc}^{-3} \text{ yr}^{-1}$, or in more “down-to-earth” units, about $\sim 23 \text{ Au}^{-3} \text{ yr}^{-1}$, i.e., about 20 X particles within a solar system-size volume per year.

In the next section I discuss three plausible specific TD processes and examine their efficacies with regard to X particle production and EHECR keeping in mind the above rough estimates of the required X particle production rate.

X Particle Production from Cosmic Strings, Monopoles, and Necklaces

Cosmic Strings

Let us first recall the salient features of evolution of cosmic strings in the Universe; for a review, see Refs. [2]. Immediately after their formation, the strings would be in a random tangled configuration. One can define a characteristic length scale, ξ_s , of the initial string

configuration in terms of the overall mass-energy density, ρ_s , of strings simply through the relation

$$\rho_s = \mu/\xi_s^2, \quad (11)$$

where μ denotes the string mass (energy) per unit length.

Initially, the strings find themselves in a dense medium, so they move under a strong frictional damping force. The damping remains significant until the temperature falls to $T \lesssim (G\mu)^{1/2}\eta$, where G is Newton's constant and η is the symmetry-breaking scale at which strings were formed. [Recall, for GUT scale cosmic strings, for example, $\eta \sim 10^{16}$ GeV, $\mu \sim \eta^2 \sim (10^{16} \text{ GeV})^2$, and $G\mu \sim 10^{-6}$.] In the friction dominated epoch, a curved string segment of radius of curvature r quickly achieves a terminal velocity $\propto 1/r$. The small scale irregularities on the strings are, therefore, quickly smoothed out. As a result, the strings are straightened out and their total length shortened. The energy density in strings, therefore, decreases with time. This means that the characteristic length scale ξ_s describing the string configuration increases with time as the Universe expands. Eventually ξ_s becomes comparable to the causal horizon distance $\sim t$. At about this time, the ambient density of the Universe becomes dilute enough that damping becomes unimportant so that the strings start moving relativistically.

Beyond this point, there are two possibilities. Causality prevents the length scale ξ_s from growing faster than the horizon length. So, either (a) ξ_s keeps up with the horizon length, i.e., ξ_s/t becomes a constant, or (b) ξ_s increases less rapidly than t .

Let us consider the second possibility first. In this case, the string density falls less rapidly than t^{-2} . On the other hand, we know that the radiation density in the radiation-dominated epoch as well as matter density in the matter-dominated epoch both scale as t^{-2} . Clearly, therefore, the strings would come to dominate the density of the Universe at some point of time. It can be shown that this would happen quite early in the history of the Universe unless the strings are very light, much lighter than the GUT scale strings. A string dominated early Universe would be unacceptably inhomogeneous conflicting with the observed Universe⁵.

The other possibility, which goes by the name of ‘‘scaling’’ hypothesis, seems to be more probable, as suggested by detailed numerical as well as analytical studies [2, 33]. The numerical simulations generally find that the string density does reach the scaling regime given by $\rho_{s,\text{scaling}} \propto 1/t^2$, and then continues to be in this regime. It is, however, clear that in order for this to happen, strings must lose energy in some form at a certain rate. This is because, in absence of any energy loss, the string configuration would only be conformally stretched by the expansion of the Universe on scales larger than the horizon so that ξ_s would only scale as the scale factor $\propto t^{1/2}$ in the radiation dominated Universe, and $\propto t^{2/3}$ in the matter dominated Universe. In both cases, this would fail to keep the string density in the scaling regime, leading back to string domination. In order for the string density to be maintained

⁵However, a string dominated *recent* Universe — dominated by ‘light’ strings formed at a phase transition at about the electroweak symmetry breaking scale — is possible. Such a string dominated recent Universe may even have some desirable cosmological properties [57]. Such light strings are, however, not of interest to us in this discussion.

in the scaling regime, energy must be lost by the string configuration per unit proper volume at a rate $\dot{\rho}_{s,\text{loss}}$ satisfying the equation

$$\dot{\rho}_{s,\text{total}} = -2\frac{\dot{R}}{R}\rho_s + \dot{\rho}_{s,\text{loss}}, \quad (12)$$

where the first term on the right hand side is due to expansion of the Universe, R being the scale factor of the expanding Universe. In the scaling regime $\dot{\rho}_{s,\text{total}} = -2\rho_s/t$, which gives $\dot{\rho}_{s,\text{loss}} = -\rho_s/t$ in the radiation dominated Universe, and $\dot{\rho}_{s,\text{loss}} = -(2/3)\rho_s/t$ in the matter dominated Universe.

The important question is, in what form does the string configuration lose its energy so as to maintain itself in the scaling regime? One possible mechanism of energy loss from strings is formation of closed loops. Occasionally, a segment of string might self-intersect by curling up on itself. The intersecting segments may intercommute, i.e., “exchange partners”, leading to formation of a closed loop which pinches off the string. The closed loop would then oscillate and lose energy by emitting gravitational radiation and eventually disappear. It can be shown that this is indeed an efficient mechanism of extracting energy from strings and transferring it to other forms. The string energy loss rate estimated above indicates that scaling could be maintained by roughly of order one closed loop of horizon size ($\sim t$) formed in a horizon size volume ($\sim t^3$) in one hubble expansion time ($\sim t$) at any time t . In principle, as far as energetics is concerned, one can have the same effect if, instead of one or few large loops, a large number of smaller loops are formed. Which one may actually happen depends on the detailed dynamics of string evolution, and can only be decided by means of numerical simulations.

Early numerical simulations seemed to support the large (i.e., \sim horizon size) loop formation picture. Subsequent simulations with improved resolution, however, found a lot of small-scale structure on strings, the latter presumably being due to kinks left on the strings after each crossing and intercommuting of string segments. Consequently, loops formed were found to be much smaller in size than horizon size and correspondingly larger in number. Further simulations showed that the loops tended to be formed predominantly on the scale of the cut-off length imposed for reasonable resolution of even the smallest size loops allowed by the given resolution scale of the simulation. It is, however, generally thought that the small-scale structure cannot continue to build up indefinitely, because the back-reaction of the kinky string’s own gravitational field would eventually stabilize the small-scale structure at a scale of order $G\mu t$. The loops would, therefore, be expected to be formed predominantly of size $\sim G\mu t$, at any time t . Although much smaller than the horizon size, these loops would still be of ‘macroscopic’ size, much larger than the microscopic string width scale ($\sim \eta^{-1} \sim \mu^{-1/2}$). These loops would, therefore, also oscillate and eventually disappear by emitting gravitational radiation. Thus, according to above picture, the dominant mechanism of energy loss from strings responsible for maintaining the string density in the scaling regime would be formation of macroscopic-size ($\gg \eta^{-1}$) loops and emission of gravitational radiation by these loops. More details of this picture of cosmic string evolution can be found in Refs. [2].

How is the above picture of cosmic string evolution relevant for cosmic rays? How does one get X particles from cosmic strings?

One way of getting X particles from cosmic strings is through the so-called cusp-evaporation mechanism [6]. I will not discuss this mechanism here, but the resulting X particle production rate generally turns out to be too low to be of relevance to EHECR.

Another possibility arises as follows: As the closed loops oscillate and emit gravitational radiation, they lose energy and shrink. Eventually, when a loop's radius shrinks to a size of order the width of the string, the string unwinds and turns into X particles, which will then decay, producing high energy particles. However, each loop in the end only produces of the order of one X particle. The resulting cosmic ray flux is again too low to be observable [9].

Clearly, the only way cosmic strings may produce large number of X particles is if macroscopic lengths of string are involved in the X particle production process. One such mechanism was suggested in Refs. [7, 8] based on the following arguments. The picture of gravitational radiation being the dominant energy loss mechanism for cosmic strings rests on the assumption that the loops themselves do not self-intersect frequently. Since the motion of a freely oscillating loop is periodic (with a period of $L/2$, L being the invariant length of the loop [58]), a loop formed in a self-intersecting configuration will undergo self-intersection within its first period of oscillation. If the loop does indeed self-intersect and break up into two smaller loops, and if the daughter loops again self-intersect breaking up into two even smaller loops, and so on, then one can see that a single initially large loop of size L can break up into a debris of tiny loops of size η^{-1} (thereby turning into X particles) within a time scale of $\sim L$. Since the largest loops are expected to be of size $< t$, one sees that the above time scale can be much smaller than one hubble time. In other words, one large loop can break up into a large number of tiny loops (X particles) within one hubble time. Such self-intersecting loops would not radiate much energy gravitationally because that would require many periods of oscillation. In other words, such repeatedly self-intersecting loops would be a channel through which energy contained in macroscopic lengths of string could go into X particles instead of into gravitational radiation. As shown in Ref. [58], some non-circular loops could also be in configurations which would collapse completely into double-line configurations and subsequently annihilate into X particles [59]. It has also been argued in Ref. [60] that the self-intersection probability of a loop increases exponentially with the number of small scale kinks on a loop.

At the time of work of Ref. [8], however, it was not clear as to what fraction of the string energy might go into X particles through processes discussed above. Treating this fraction to be a free parameter f , i.e., assuming that a fraction f of the energy extracted from the long strings per unit volume per unit time went into X particles, the authors of Ref. [8] found that the fraction f had to be rather small, $f \lesssim 7 \times 10^{-4}$; otherwise, the predicted cosmic ray flux from GUT scale cosmic strings would exceed the observed flux. Results of more recent calculation of the predicted observable particle flux [16] (see Fig. 1) correspond to an upper limit on f which is about two orders of magnitude lower⁶.

⁶This is due to the fact that the 'observable' particle flux now includes the gamma ray flux in addition to the protons — in contrast to only the much lower proton flux considered in Ref. [8] — and also because

The actual value of f is still unknown. But if gravitational radiation, and not massive particle radiation, is the dominant energy loss mechanism for cosmic strings, then the fraction f may actually be much smaller than the above upper limit, in which case the flux of cosmic rays produced by cosmic strings through X particles would be small and below the observed flux. However, rapid conversion of a significant fraction of the energy in macroscopically large loops into tiny loops (X particles) through repeated loop self-intersections due, for example, to the presence of large number of kinks on the loops [60], and consequent production of significant EHECR flux, cannot be ruled out.

Very recently, the notion gravitational radiation as the dominant energy loss mechanism for cosmic strings has been questioned by the results of new numerical simulations of evolution of cosmic strings [33]. Authors of Ref. [33] claim that if loop production is not artificially restricted by imposing a cutoff length for loop size in the simulation, then loops tend to be produced dominantly on the smallest allowed length scale in the problem, namely, on the scale of the width of the string. Such small loops promptly collapse into X particles. In other words, there is essentially no loop production at all — the string energy density is maintained in the scaling regime by energy loss from strings predominantly in the form of direct X particle emission, rather than by formation of large loops and their subsequent gravitational radiation. This new result, while subject to confirmation by independent simulations, obviously has important implications for EHECR. Indeed, in this case, the upper limit on the fraction f mentioned above implies severe constraint on GUT-scale cosmic strings. From the results of Ref. [33], the string energy density in the scaling regime is $\rho_{s,\text{scaling}} \simeq \mu/(0.3t)^2$. With X particle production as the dominant energy loss mechanism, we immediately see from Eq. (12) that rate of production of X particles from strings per unit volume must be $dn_X/dt \simeq 7.4(\mu/m_X)t^{-3}$ in the matter dominated era. Taking, for cosmic strings, $\mu \simeq \pi\eta^2$, and taking $m_X \sim 0.7\eta$, where η is the symmetry-breaking scale, we get by using the constraint imposed by Eq. (10), $\eta \lesssim 4.2 \times 10^{13}$ GeV. Thus the GUT scale cosmic strings with $\eta \sim 10^{16}$ GeV are ruled out by EHECR data if the results of Ref. [33] are correct. At the same time X particles from cosmic strings formed at a phase transition with $\eta \sim 10^{13} - 10^{14}$ GeV are able to explain the EHECR data. Cosmic strings may thus be a “natural” source of extremely high energy cosmic rays if massive particle radiation, and *not* gravitational radiation, is indeed their dominant energy loss mechanism.

Cosmic string formation with $\eta \sim 10^{14}$ GeV rather than at the GUT scale of $\sim 10^{16}$ GeV is not hard to envisage. For example, the symmetry breaking scheme $\text{SO}(10) \rightarrow \text{SU}(3) \times \text{SU}(2) \times \text{U}(1)_Y \times \text{U}(1)$ can take place at the GUT unification scale $M_{\text{GUT}} \sim 10^{16}$ GeV; with no U(1) subgroup broken, this phase transition produces no strings. However, the second U(1) can be subsequently broken with a second phase transition at a scale $\sim 10^{14}$ GeV to yield the cosmic strings relevant for EHECR. Note that these strings would be too light to be relevant for structure formation in the Universe and their signature on the CMBR sky would also be too weak to be detectable. Instead, the extremely high energy end of the cosmic ray spectrum may offer a probing ground for signatures of these cosmic strings.

of the maximum likelihood normalization of the predicted flux to the observed data.

Monopoles

If monopoles were formed at a phase transition in the early Universe, then, as Hill [4] suggested in 1983, a metastable monopole-antimonopole bound state — “monopolonium” — is possible. At any temperature T , monopolonia would be formed with binding energy $E_b \gtrsim T$. The initial radius r_i of a monopolonium would be $r_i \sim \frac{1}{2}g_m^2/E_b$, where g_m is the magnetic charge (which is related to the electronic charge e through the Dirac quantization condition $eg_m = N/2$, N being the monopole’s winding number). Classically, of course, the monopolonium is unstable. Quantum mechanically, the monopolonium can exist only in certain “stationary” states characterized by the principal quantum number n given by $r = n^2 a_m^B$, where n is a positive integer, r is the instantaneous radius, and $a_m^B = 8\alpha_e/m_M$ is the “magnetic” Bohr radius of the monopolonium. Here $\alpha_e = 1/137$ is the “electric” fine-structure constant, and m_M is the mass of a monopole. Since the Bohr radius of a monopolonium is much less than the Compton wavelength (size) of a monopole, i.e., $a_m^B \ll m_M^{-1}$, the monopolonium does not exist in the ground ($n = 1$) state, because the monopole and the antimonopole would be overlapping, and so would annihilate each other. However, a monopolonium would initially be formed with $n \gg 1$; it would then undergo a series of transitions through a series of tighter and tighter bound states by emitting initially photons and subsequently gluons, Z bosons, and finally the GUT X bosons. Eventually, the cores of the monopole and the antimonopole would overlap, at which point the monopolonium would annihilate into X particles. Hill showed that the life time of a monopolonium is proportional to the cube of its initial radius. Depending on the epoch of formation, some of the monopolonia formed in the early Universe could be surviving in the Universe today, and some would have collapsed in the recent epochs. It can be shown [10] that monopolonia collapsing in the present epoch would have been formed in the early Universe at around the epoch of primordial nucleosynthesis.

The X particles produced by the collapsing monopolonia may give rise to EHECR. This possibility was studied in details in Ref. [10], who showed that this process, like cosmic strings, can also be described by an equation for X particle production rate described by Eq. (1) with $p = 1$. The efficacy of the process, however, depends on two parameters, namely, (a) the monopolonium-to-monopole fraction at formation (ξ_f) and (b) the monopole abundance. The latter is unknown, while the former is in principle calculable by using the classical Saha ionization formalism. However, phenomenologically, since a monopole mass can be typically $m_M \sim 40m_X$ (so that each monopolonium collapse can release ~ 80 X particles), we see from Eq. (10) that one requires roughly (only!) about 3 monopolonium collapse per decade within a volume roughly of the size of the solar system. Whether or not this can happen depends, as already mentioned, on ξ_f as well as on the monopole abundance, the condition [10] being $(\Omega_M h_{100}^2)h_{100}\xi_f \simeq 1.7 \times 10^{-8}(m_X/10^{16} \text{ GeV})^{1/2}(10 \text{ Mpc}/\lambda_{\gamma,300})$, where Ω_M is the mass density contributed by monopoles in units of closure density of the Universe, and h_{100} is the present hubble constant in units of $100 \text{ km sec}^{-1} \text{ Mpc}^{-1}$. Thus, as expected, larger the monopole abundance, smaller is the monopolonium fraction ξ_f required to explain the EHECR flux. Note that, since ξ_f must always be less than unity, the above requirements can be satisfied as long as $(\Omega_M h_{100}^2)h_{100} > 1.7 \times 10^{-8}(m_X/10^{16} \text{ GeV})^{1/2}$. Recall, in this

context, that the most stringent bound on the monopole abundance is given by the Parkar bound [29], $(\Omega_M h_{100}^2)_{\text{Parkar}} \lesssim 4 \times 10^{-3} (m_M/10^{16} \text{ GeV})^2$. The estimate of ξ_f obtained by using the Saha ionization formalism [4, 10] shows that the resulting requirement on the monopole abundance (in order to explain the EHECR flux) is well within the Parkar bound mentioned above. The monopolonium collapse, therefore, seems to be an attractive scenario in this regard. A detailed numerical simulation of monopolonium formation to determine the monopolonium fraction at formation would, however, be useful in this context.

Necklaces

A cosmic necklace is a possible hybrid topological defect consisting of a closed cosmic string loop with monopole “beads” on them. Such a hybrid defect was first considered by Hindmarsh and Kibble [61]. Such defects could be formed in a two stage symmetry-breaking scheme such as $G \rightarrow H \times U(1) \rightarrow H \times Z_2$, where Z_2 is the discrete group $\{-1,1\}$ under multiplication. In such a symmetry breaking, monopoles are formed at the first step of the symmetry breaking if the group G is semisimple. In the second step, the so-called “ Z_2 ” strings are formed and then each monopole gets attached to two strings, with the monopole magnetic flux channeled along the strings. Possible production of massive X particles from necklaces has been pointed out in Ref. [11].

The evolution of the necklace system is not well understood. The crucial quantity is the dimensionless ratio $r \equiv m_M/(\mu d)$, where m_M denotes the monopole mass, μ is the string mass per unit length, and d is the average separation between the monopoles. For $r \ll 1$, the monopoles play a subdominant role, and the evolution of the system is similar to that of ordinary cosmic strings. For $r \gg 1$, on the other hand, the monopoles determine the behavior of the system. The monopoles sitting on the strings tend to make the motion of the closed necklaces aperiodic. The authors of Ref. [11] assume that closed necklaces undergo frequent self-intersections, leading to monopole - antimonopole annihilation and, consequently, release of massive X particles. The X particle production rate for the necklace system can also be written in the form of Eq. (1) with $p = 1$. The efficacy of the process depends on free parameters, r , μ and m_M . For appropriate choice of the parameters, the required EHECR flux can be obtained. For more details see Ref. [11] and the article by Berezhinsky in this volume.

Topological Defects in Supersymmetric Theories

Recently, it has been pointed out [62] that in a wide class of supersymmetric unified theories, the higgs bosons associated with the gauge symmetry breaking can be ‘light’ — of mass of order the soft supersymmetry breaking scale $\sim \text{TeV}$ — even though the gauge symmetry breaking scale (and hence the mass of the gauge boson) itself may be much larger. The topological defects in these theories can, therefore, simultaneously be sources of $\sim \text{TeV}$ mass-scale higgs bosons as well as supermassive (mass up to $\sim 10^{16} \text{ GeV}$) gauge bosons. The decay of the TeV higgs may give a significant contribution to the observed diffuse γ -ray

background above a few GeV, while the supermassive gauge boson decay may explain the EHECR. For more details, see Ref. [62].

Conclusion

There is no dearth of specific models of X particle producing processes involving topological defects. Almost all the “realistic” processes studied so far can be parametrized in the form of Eq. (1) with $p = 1$. The spectra of various kinds of particles produced for all these processes would essentially be similar to the ones shown in Fig. 1. Different processes might, however, contribute different amounts to the total flux. It is difficult to say which particular process may contribute most to the observed EHECR flux. However, in this respect, the cosmic string scenario seems to be relatively parameter free, especially if the new results of Ref. [33] are correct. Experimentally, it will be difficult, if not impossible, to tell which specific TD process, if at all, is responsible for the EHE cosmic rays. The best one can hope for is that proposed future experiments like OWL, Auger, and so on, may be able to tell us whether topological defects (or, for that matter, any *non-acceleration* mechanism in general) or some other completely different scenario is involved in producing the observed EHECR. In any event, the prospect of being able to look for signatures of new physics with the proposed EHECR experiments is certainly exciting, to say the least.

Note added: Recently it has been pointed out [63] that if indeed decays of X particles from TD processes are responsible for the EHECR, then the same TD processes occurring in the early Universe may also have given rise to the observed baryon asymmetry of the Universe through CP- and Baryon number violating decays of the X particles.

Acknowledgments

I am grateful to Günter Sigl for many helpful discussions, and in particular for providing the Figure. This work is supported by a NAS/NRC Resident Senior Research Associateship at NASA/GSFC.

References

- [1] T.W.B. Kibble, *J. Phys.* **A9**, 1387 (1976).
- [2] A. Vilenkin and E.P.S. Shellard, *Cosmic Strings and other Topological Defects* (Cambridge Univ. Press, Cambridge, 1994); M. Hindmarsh and T. W. B. Kibble, *Rep. Prog. Phys.* **58**, 477 (1995); T. W. B. Kibble, *Aust. J. Phys.* **50**, 697 (1997); T. Vachaspati, *Topological Defects in the Cosmos and Lab* (hep-ph/9802311) (to appear in *Contemporary Physics*).
- [3] P. Bhattacharjee, C.T. Hill, and D.N. Schramm, *Phys. Rev. Lett.* **69**, 567 (1992).

- [4] C.T. Hill, *Nucl. Phys.* **B 224**, 469 (1983).
- [5] C.T. Hill, D.N. Schramm, and T.P. Walker, *Phys. Rev.* **D 36**, 1007 (1987).
- [6] J. H. MacGibbon and R. H. Brandenberger, *Nucl. Phys.* **B 331**, 153 (1990); P. Bhattacharjee, *Phys. Rev.* **D 40**, 3968 (1989); M. Mohazzab and R. Brandenberger, *Int. Jour. Mod. Phys.* **D 2**, 183 (1993).
- [7] P. Bhattacharjee, in *Astrophysical Aspects of the Most Energetic Cosmic Rays*, eds. M. Nagano and F. Takahara (World Scientific, Singapore, 1991), pp. 382 – 399.
- [8] P. Bhattacharjee and N.C. Rana, *Phys. Lett.* **B 246**, 365 (1990).
- [9] A. J. Gill and T. W. B. Kibble, *Phys. Rev.* **D 50**, 3660 (1994).
- [10] P. Bhattacharjee and G. Sigl, *Phys. Rev.* **D 51**, 4079 (1995).
- [11] V. Berezhinsky and A. Vilenkin, *Phys. Rev. Lett.* **79**, 5202 (1997).
- [12] D.J. Bird *et al*, *Phys. Rev. Lett.* **71**, 3401 (1993); *Astrophys. J.* **441**, 144 (1995); N. Hayashida *et al*, *Phys. Rev. Lett.* **73**, 3491 (1994); S. Yoshida *et al*, *Astropart. Phys.* **3**, 105 (1995).
- [13] G. Sigl, D.N. Schramm, and P. Bhattacharjee, *Astropart. Phys.* **2**, 401 (1994).
- [14] G. Sigl, S. Lee, D. N. Schramm, and P. Bhattacharjee, *Science*, **270**, 1977 (1995).
- [15] G. Sigl, S. Lee, and P. Coppi, *astro-ph/9604093*.
- [16] G. Sigl, S. Lee, D. N. Schramm, and P. Coppi, *Phys. Lett.* **B 392**, 129 (1997).
- [17] R.J. Protheroe and T. Stanev, *Phys. Rev. Lett.* **77**, 3708 (1996); **78**, 3420 (1997) (E).
- [18] A. M. Hillas, *Ann. Rev. Astron. Astrophys.* **22**, 425 (1984).
- [19] C.A. Norman, D.B. Melrose, and A. Achterberg, *Astrophys. J.* **454**, 60 (1995).
- [20] See, e.g., L. O’C Drury, *Rep. Prog. Phys.* **46**, 973 (1983); F. C. Jones and D. C. Ellison, *Sp. Sci. Rev.* **58**, 259 (1991).
- [21] J.P. Rachen and P.L. Biermann, *Astron. Astrophys.* **272**, 161 (1993); P. L. Biermann, in this volume.
- [22] J. W. Elbert, and P. Sommers, *Astrophys. J.* **441**, 151 (1995).
- [23] P. Bhattacharjee, in *Non-Accelerator Particle Physics*, Ed. R. Cowsik (World Scientific, Singapore, 1995).

- [24] P. Bhattacharjee, in *Extremely High Energy Cosmic Rays: Astrophysics and Future Observatories*, Ed. M. Nagano (ICRR, Univ. of Tokyo, 1996).
- [25] G. Sigl, *Sp. Sci. Rev.* **75**, 375 (1996).
- [26] F.A. Aharonian, P. Bhattacharjee, and D.N. Schramm, *Phys. Rev.* **D 46**, 4188 (1992).
- [27] S. Yoshida, *Astropart. Phys.* **2**, 187 (1994); S. Yoshida, H. Dai, C. Jui, and P. Sommers, *Astrophys. J.* **479**, 547 (1997).
- [28] X. Chi, C. Dahanayake, J. Wdowczyk, and A. W. Wolfendale, *Astropart. Phys.* **1**, 129 (1993); *ibid.* **1**, 239 (1993).
- [29] E.W. Kolb and M.S. Turner, *The Early Universe* (Addison-Wesley, Redwood City, California, 1990).
- [30] C. Bäuerle *et al*, *Nature* **382**, 332 (1996); V. Ruutu *et al*, *Nature* **382**, 334 (1996).
- [31] W.H. Zurek, *Nature* **317**, 505 (1985).
- [32] E. Witten, *Nucl. Phys.* **B 249**, 557 (1985).
- [33] G. Vincent, N.D. Antunes, and M. Hindmarsh, *Phys. Rev. Lett.* (to be published) (hep-ph/9708427); G. R. Vincent, M. Hindmarsh, and M. Sakellariadou, *Phys. Rev.* **D 56**, 637 (1997).
- [34] K. Greisen, *Phys. Rev. Lett.* **16**, 748 (1966); G. T. Zatsepin and V. A. Kuzmin, *Pisma Zh. Eksp. Teor. Fiz.* **4**, 114 (1966) [*JETP. Lett.* **4**, 78 (1966)]; F. W. Stecker, *Phys. Rev. Lett.* **21**, 1016 (1968); F. A. Aharonian and J. W. Cronin, *Phys. Rev.* **D 50**, 1892 (1994).
- [35] B. Andersson *et al*, *Phys. Rep.* **97**, 31 (1983).
- [36] G. Marchesini and B.R. Webber, *Nucl. Phys.* **B 310**, 461 (1988); G. Marchesini *et al*, *Comp. Phys. Comm.* **67**, 465 (1992); HERWIG version 5.9, hep-ph/9607393.
- [37] T. Sjöstrand and M. Bengtsson, *Comp. Phys. Comm.* **43**, 367 (1987).
- [38] L. Lönnblad, *Comp. Phys. Comm.* **71**, 15 (1992).
- [39] Ya. I. Azimov, Yu. L. Dokshitzer, V. A. Khoze, and S. I. Troyan, *Z. Phys.* **C 27**, 65 (1985); **C 31**, 213 (1986).
- [40] Yu. L. Dokshitzer, V. A. Khoze, A. H. Mueller, and S. I. Troyan, *Basics of perturbative QCD* (Editions Frontiers, Saclay, 1991); R. K. Ellis, W. J. Stirling, and B. R. Webber, *QCD and Collider Physics* (Cambridge Univ. Press, Cambridge, England, 1996); V. A. Khoze and W. Ochs, *Int. J. Mod. Phys.* (To be published) (hep-ph/9701421).
- [41] A.H. Mueller, *Nucl. Phys.* **B213**, 85 (1983); *ibid.* **B241**, 141 (1984) (E).

- [42] F.W. Stecker, *Astrophys. J.* **228**, 919 (1979).
- [43] A. Chen, J. Dwyer, and P. Kaaret, *Astrophys. J.* **463**, 169 (1996).
- [44] P. Sreekumar *et al*, *Astrophys. J.* **494** (1998) (in press) (astro-ph/9709257); P. Sreekumar, F. W. Stecker, and S. C. Kappadath, astro-ph/9709258 (in press).
- [45] M.H. Salamon and F.W. Stecker, *Astrophys. J.* (1998) (in press); astro-ph/9704166.
- [46] P. S. Coppi and F. A. Aharonian, *Astrophys. J.* **487**, L9 (1997).
- [47] T.J. Weiler, *E-print* hep-ph/9710431.
- [48] P. Lipari, *Astropart. Phys.* **1**, 195 (1993).
- [49] W. Rhode *et al.*, *Astropart. Phys.* **4**, 217 (1996).
- [50] M. Aglietta *et al*, in *Proc. 24th Int. Cosmic Ray Conf.* **1**, 638 (1995).
- [51] R.M. Baltrusaitis *et al*, *Astrophys. J.* **281**, L9 (1984); *Phys. Rev.* **D 31**, 2192 (1985).
- [52] G. Parente and E. Zas, *E-print* astro-ph/9606091.
- [53] G. Sigl, K. Jedamzik, D. N. Schramm, and V. Berezhinsky, *Phys. Rev.* **D 52**, 6682 (1995).
- [54] F.W. Stecker, C. Done, M. H. Salamon, and P. Sommers, *Phys. Rev. Lett.* **66**, 2697 (1991); **69**, 2738 (1992) (E).
- [55] R. Gandhi, C. Quigg, M.H. Reno, and I. Sarcevic, *Astropart. Phys.* **5**, 81 (1995).
- [56] J.J. Blanco-Pillado, R.A. Vazquez, and E. Zas, *Phys. Rev. Lett.* **78**, 3614 (1997).
- [57] A. Vilenkin, *Phys. Rev. Lett.* **53**, 1016 (1984); D. Spergel and Ue-Li Pen, *Astrophys. J.* **491**, L67 (1997).
- [58] T.W.B. Kibble and N. Turok, *Phys. Lett.* **B 116**, 141 (1982).
- [59] P. Bhattacharjee, T.W.B. Kibble and N. Turok, *Phys. Lett.* **B 119**, 95 (1982).
- [60] X.A. Siemens and T.W.B. Kibble, *Nucl. Phys.* **B 438**, 307 (1995).
- [61] M.B. Hindmarsh and T.W.B. Kibble, *Phys. Rev. Lett.* **55**, 2398 (1985).
- [62] P. Bhattacharjee, Q. Shafi, and F.W. Stecker, *E-print* hep-ph/9710533.
- [63] P. Bhattacharjee, *E-print* hep-ph/9803223.